

University of Mississippi

eGrove

Honors Theses


Honors College (Sally McDonnell Barksdale
Honors College)

Spring 5-12-2023

Development of Novel Sensor Coating Methodology to Enable Understanding of Fouling Mechanisms on Ion Exchange Membranes

Andrew Ulmer

Follow this and additional works at: https://egrove.olemiss.edu/hon_thesis

 Part of the [Membrane Science Commons](#), [Polymer and Organic Materials Commons](#), and the [Transport Phenomena Commons](#)

Recommended Citation

Ulmer, Andrew, "Development of Novel Sensor Coating Methodology to Enable Understanding of Fouling Mechanisms on Ion Exchange Membranes" (2023). *Honors Theses*. 2866.
https://egrove.olemiss.edu/hon_thesis/2866

This Undergraduate Thesis is brought to you for free and open access by the Honors College (Sally McDonnell Barksdale Honors College) at eGrove. It has been accepted for inclusion in Honors Theses by an authorized administrator of eGrove. For more information, please contact egrove@olemiss.edu.

Development of Novel Sensor Coating Methodology to Enable Understanding of
Fouling Mechanisms on Ion Exchange Membranes

By
Andrew Jacob Ulmer

A thesis submitted to the faculty of The University of Mississippi in partial fulfillment of the
requirements of the Sally McDonnell Barksdale Honors College.

Oxford
May 2023

Approved by:

Advisor: Dr. Alexander M. Lopez

Reader: Dr. Thomas Werfel

Reader: Dr. John H. O'Haver

© 2023
Andrew Jacob Ulmer
ALL RIGHTS RESERVED

Acknowledgments

First and foremost, I would like to express my sincere gratitude to my thesis advisor, Dr. Alexander Lopez, whose constant guidance and encouragement helped shape the trajectory of this project and significantly facilitated my growth as an undergraduate researcher. I would also like to thank The University of Mississippi's Department of Chemical Engineering for providing the necessary space and resources to conduct my research.

Secondly, I would like to thank Dr. Brenda Hutton-Prager for allowing me access and training to use the QCM-D. Additionally, I would like to thank a graduate alum from the UM Chemical Engineering Department, John Malone, for training me on research protocols and providing additional guidance throughout the initial stages of this research project.

Finally, I would like to thank the Sally McDonnell Barksdale Honors College for providing numerous resources and opportunities to cultivate my academic growth in and outside the classroom. I also want to express my appreciation to my thesis committee for the time and effort they dedicated to reading and providing feedback for this manuscript.

Abstract

ANDREW JACOB ULMER: Development of Novel Sensor Coating Methodology to Enable Understanding of Fouling Mechanisms on Ion Exchange Membranes
(Under the direction of Dr. Alexander M. Lopez)

As populations expand and natural water resources are depleted, severe droughts and limited access to clean water have become an increased threat to areas across the world. Effective and economic water treatment methods such as electrodialysis (ED) are vital for combating these threats, especially in developing nations and secluded locations. Organic foulant adsorption on the surface of ion exchange membranes severely limits the capabilities of water desalination systems such as ED along with significantly increasing maintenance costs. Understanding characteristics such as the total amount and rate at which these foulants at specific concentrations adsorb and desorb to the membranes is paramount for improving system process performance. To observe the precise rate of fouling for two foulants commonly used in experimentation: sodium alginate (SA) and bovine serum albumin (BSA), this study proposed employing the quartz crystal microbalance with dissipation monitoring (QCM-D) due to its precise, real-time measurement of surface interactions. The procedure for developing a mock ion-exchange membrane on the surface of a gold QCM-D sensor was developed and various techniques were used to validate the formation of the membrane layer such as atomic force microscopy (AFM) and contact angle (CA) analysis. The validation results signify that out of the methods applied, increasing the amount of applied coating solution from 150 to 300 drops caused the development of a more uniform mock ion exchange membrane (IEM) layer. Furthermore, drying the sensors in an oven at 60°C between coating reduced material clustering and thus decreased the average roughness (R_a) value. This novel coating methodology is highly adaptable and could streamline the development and testing of case-specific feedwater foulant profiles, anti-foulant coatings, and effective cleaning procedures.

TABLE OF CONTENTS

TABLE OF FIGURES	vi
LIST OF ABBREVIATIONS.....	vii
Chapter I: Introduction.....	1
Overview of Electrodialysis Systems	1
Current Challenges and Preventative Measures for Organic Fouling	2
Overview of Quartz Crystal Microbalance (QCM) System	3
Materials and Methods	5
Chapter II: Results and Discussion.....	8
ED Experimentation with Sodium Alginate and Bovine Serum Albumin	8
Development of IEM on Gold QCM-D Sensor	12
Visualization and Validation of Mock IEM	15
Preliminary QCM-D Experimentation with Uncoated Sensors	19
Chapter III: Conclusion and Future Work	20
LIST OF REFERENCES	23
LIST OF EQUATIONS	25
APPENDIX.....	26

TABLE OF FIGURES

Figure 1: Electrodialysis Separation Diagram	1
Figure 2: QCM-D Analysis Diagram	5
Figure 3: Experimental Set Up for Electrodialysis Experimentation	6
Figure 4: Change in conductivity of Diluate Solutions with the Addition of Foulants	9
Table 1: Current Efficiency Results from Electrodialysis Experimentation	10
Figure 5: Change in Conductivity of Diluate Solutions from Previous Study	11
Figure 6: Change in Mass of QCM-D Sensors throughout Coating Procedure	13
Figure 7: Images of QCM-D Sensor Surfaces after Coating at 250x Magnification	14
Figure 8: 5x5 μm and 20x20 μm AFM Scan of Coated QCM-D Sensors	15
Figure 9: Surface Roughness Analysis using Gwyddion Software	17
Table 2: Average Surface Roughness Values for Coated QCM-D Sensors	18
Figure 10: Contact Angle Measurements of Coated QCM-D Sensors	19
Figure 11: Preliminary QCM-D Experimentation with Neat Sensors	20
Figures 12-15	Appendix

LIST OF ABBREVIATIONS

CEM	Cation Exchange Membranes
AEM	Anion Exchange Membranes
ED	Electrodialysis
SA	Sodium Alginate
BSA	Bovine Serum Albumin
AFM	Atomic Force Microscopy
FTIR	Fourier Transform Infrared Spectroscopy
NMR	Nuclear Magnetic Resonance
QCM-D	Quartz Crystal Microbalance with Dissipation Monitoring
R _a	Roughness Average
DI	Distilled

Chapter I: Introduction

Overview of Electrodialysis Systems

Electrodialysis is a technique that separates charged particles, such as ions, from a feed water system using an electrical potential gradient as the driving force. This separation is achieved through a series of alternating cation exchange membranes (CEM) and anion exchange membranes (AEM), referred to as a stack. CEMs have negatively charged surfaces, while AEMs have positively charged surfaces resulting in selective permeability of cations and anions, respectively. Solutions flow through channels in spacers between each membrane, and the electrical current draws cations toward the cathode and anions toward the anode, as shown in **Fig. 1**. This process results in a deionized solution called the dilute stream, and an ionized solution called the concentrate or brine stream. Often rinse solutions are utilized to neutralize the concentrated ion streams and facilitate the fluid byproduct disposal process.

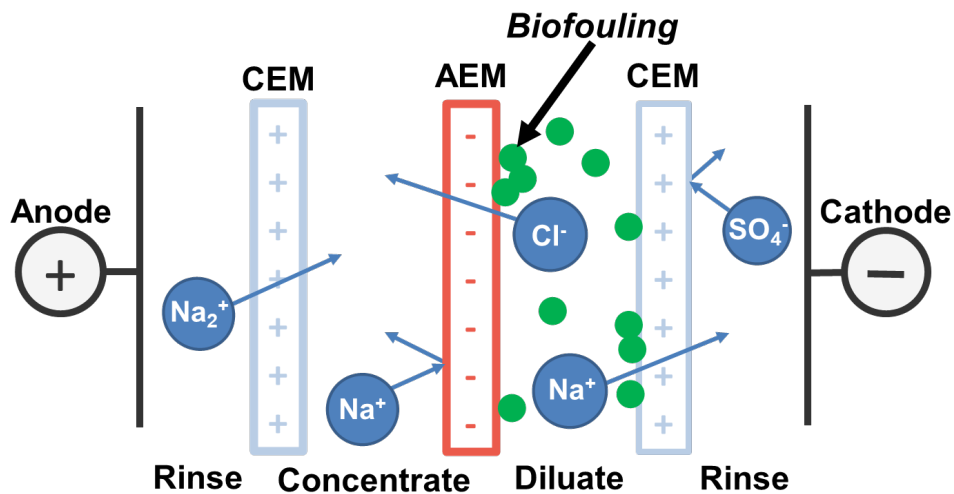


Figure 1: Diagram representing the movement of ions across exchange membranes in Electrodialysis Systems. As these ions permeate, organic particles in the solution adhere to the membrane surface or become lodged within membrane pores, known as fouling.

Electrodialysis (ED) is a well-established and reliable system that provides an effective and sustainable method of ion separation. This system is used for various processes such as desalination of salt water, wastewater treatment, purification of brackish water, pharmaceutical production, and development of food and beverage products [1]. Parameters such as polymer density, structural morphology, and surface charge have been altered to achieve variation in membrane properties [2]. The most desired properties are high permselectivity, low electrical resistance, and low manufacturing cost. Much research has been conducted to improve ED systems' properties; however, organic fouling still significantly hinders the efficiency of these systems over time.

Current Challenges and Preventative Measures for Organic Fouling

Increasing understanding of foulant characteristics on the surface of ion exchange membranes (IEMs) is paramount to developing and validating anti-foulant layers and specified cleaning procedures. Furthermore, these developments are vital for maximizing the system's efficiency by increasing membrane operation life and decreasing maintenance costs. High concentrations of organic particles in the feed water often cause significant complications for industries utilizing IEMs as these particles deposit on the membrane's surface and clog pores. Without the proper preventative measures, fouling can gradually reduce system performance by causing a decrease in separation efficiency, higher energy consumption, and even irreversible membrane degradation [3]. In these industries, cleaning procedures or membrane replacement costs can range from 20 – 30% to 40 – 50% of total operating expenses for pressure-driven and electro-membrane processes [4]. For the scope of this research, we focused on the latter utilized in economic and widespread electrodialysis (ED) systems.

Current preventative measures for fouling include applying pre-treatments, controlling operational conditions such as flow rate and temperature, and performing routine cleanings.

However, proper foulant identification and characterization are vital for selecting the most effective preventative techniques and cleaning procedures [5]. Foulant identification is also imperative for developing new anti-foulant methods and research. Membrane autopsies are commonly performed on fouled membranes utilizing various tools, including atomic force microscopy (AFM), Fourier transform infrared spectroscopy (FTIR), and nuclear magnetic resonance (NMR). These methods have been proven moderately effective but are often destructive and expensive [6]. They also do not allow for real-time analysis of foulant layer characteristics. New non-destructive methods for fouling analysis are imperative to enhance scientists' understanding of fouling mechanisms and develop solutions to minimize foulant layer formation during operation.

Overview of Quartz Crystal Microbalance (QCM) System

This research proposed using the quartz crystal microbalance with dissipation monitoring (QCM-D) to better analyze surface-interaction phenomena and identify foulant layer properties in ED systems. The QCM-D is capable of obtaining highly accurate, real-time measurements of mass changes on the surface of a sensor along the nanoscale. The fundamentals of this device are built on the piezoelectric effect expressed by specific materials such as quartz. This effect causes the generation of an electrical charge in response to mechanical stress or strain. Conversely, these materials produce a mechanical force or vibration in response to an electrical charge.

In the QCM-D system, there are chambers each containing a thin quartz crystal disk that is supplied with an electrical current by two electrodes on opposite sides of the disk, producing a constant resonance frequency. Directly above this crystal lies a sensor whose initial mass and thickness determine this initial resonance frequency. A solution can then be run over the surface of the sensor. As particles in the solution absorb and desorb on the sensor's surface, mechanical forces are applied to the crystal, as illustrated in **Fig. 2**. The resulting changes in resonance

frequency can be collected and analyzed by the device to determine the change in mass using the Sauerbrey relation:

$$\Delta m = -C \times \frac{\Delta f}{n} \quad (1)$$

This equation expresses the linear relationship between the change in frequency and mass in QCM-D experimentation. Variable C refers to the piezoelectric material's mass-sensitivity constant and is defined as the amount of material (ng) per cm^2 of the sensor required to increase the resonance frequency 1Hz. The following equation determines this constant:

$$C = \frac{v_q \times \rho_q}{2(f_0)^2} \quad (2)$$

In this equation, v_q refers to the shear wave velocity, ρ_q is the density of the piezoelectric material, and f_0 is the fundamental resonance frequency [7]. The variable n represents the chosen harmonic frequency. These harmonics or overtones are multiples of the base resonance frequency ($n=1$). Increasing the frequency allows additional information about the viscoelastic properties of the subject material on the sensor's surface to be collected. The Sauerbrey equation is only valid if the material layer on the sensor is relatively thin and firmly bonded to the surface.

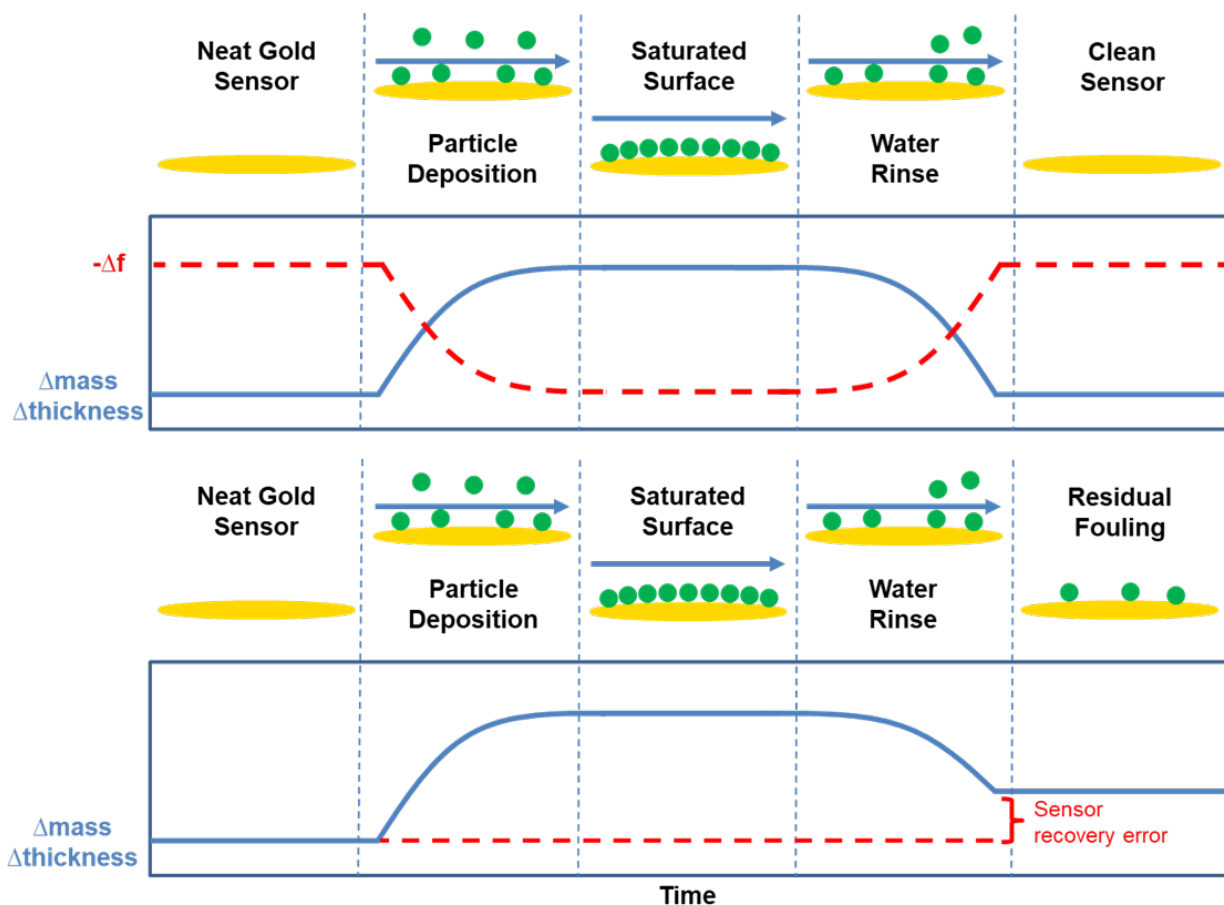


Figure 2: Diagram illustrating the measurement process throughout QCM-D experimental procedures. As particles precipitate out of the solution and adhere to the sensor's surface, the mass change increases resonance frequency. Once the surface is saturated, the frequency reaches a steady state, and the total thickness of the particle layer can be calculated. Rinse solutions are often used to recover the sensor by removing adhered particles.

Materials and Methods

Commercial Fumion® FAA3-SOLUT-10 solution of 8-12wt% anion exchange membrane polymer dissolved in N-methyl-2-pyrrolidone (NMP) was purchased from FuMA-Tech. This solution was diluted in distilled (DI) water to 0.1wt% and used as the coating medium. QSX 301 Gold (Au) QCM-D sensors with a surface roughness value of 1nm Root Mean Square (RMS) were purchased from Biolin Scientific. Biolin Scientific also supplied the cleaning and preparation solutions for the QCM-D gold sensors. The model foulants, sodium

alginate (SA, C₆H₇O₆Na) and bovine serum albumin (BSA) were stored in the fridge at ~4°C and at room temperature (~20°C), respectively.

ED filtration was performed using a scaled system to collect current efficiency data and analyze the effect of adding two chosen compounds: SA and BSA. These compounds have been utilized in previous filtration studies as model foulants for proteins and polysaccharides commonly found in wastewater sources [8, 9]. A Materflex® peristaltic pump generated the necessary pressure for constant fluid flow, and a GW Instek GPS-3030DD DC power supply established the electrical gradient. A simple IEM stack was used for ED filtration consisting of two CEMs, one AEM, two spacers for the rinse solution, one spacer for the concentrate solution, and one spacer for the diluate solution. See **Fig. 3** for the experimental setup.

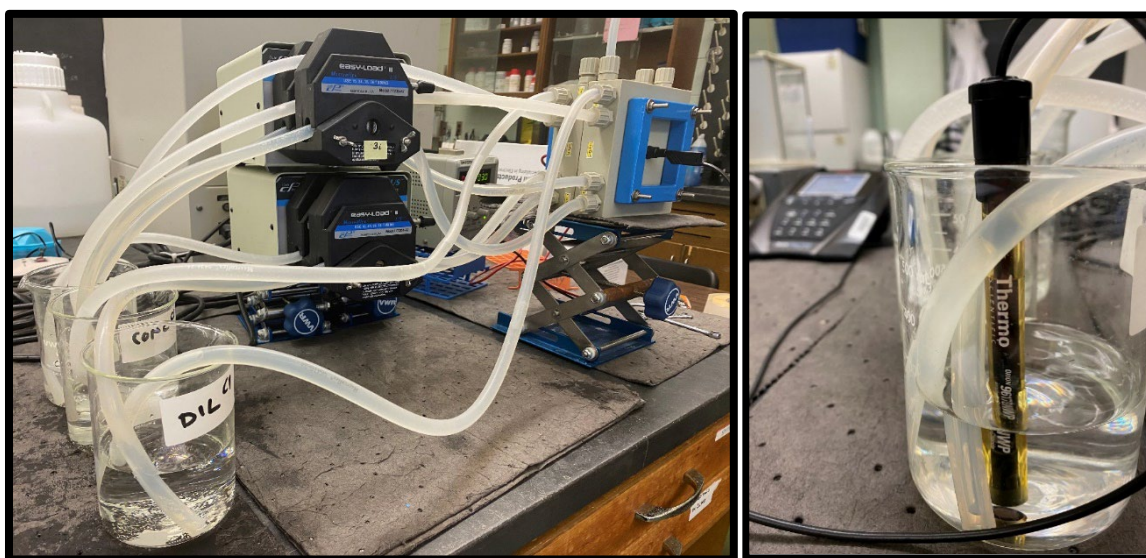


Figure 3: (Left) The experimental setup for ED filtration analysis. (Right) A conductivity probe was placed in the diluate solution to determine the current efficiency, and measurements were taken over time.

By measuring the initial ion concentration in mol per liters (C_i) and the final ion concentration (C_f) over a separation time in hours (s), the current efficiency of the system was determined using the following equation:

$$\xi = \frac{zFV \times (C_i - C_f)}{t \times I} = \frac{\text{energy consumed}}{\text{energy supplied}} \quad (3)$$

The ion valence (z) was assumed to be one, and Faraday's Constant (F) equals 96487 C/mol. The diluate volume (V) and average current in amps from the DC power supply (I) were measured for each experiment.

Previous studies have used the QCM-D to monitor the deposition and removal of foulants in membrane bioreactor systems and on stainless steel surfaces [10, 11]. To adapt this concept for QCM-D experimentation relating to ED systems, we first developed a methodology for building a mock IEM on the surface of a gold QCM-D sensor. This was achieved by spin coating the Fumion solution on four separate clean sensors with slight variations to the technique. One hundred fifty drops of the solution were applied to the first two sensors in 30-drop increments, followed by drying overnight at either room temperature or in an oven at 60C. This process was repeated for the following two sensors, but the number of applied drops was increased to 300. To validate the formation of the IEM and determine any variation in the results for the four techniques, the surfaces of the sensors were observed and analyzed using a Keyence microscope, AFM, and CA measurements. Through the development and validation of this methodology, we have shown the potential of the QCM-D to become a valuable tool for foulant identification and characterization. Furthermore, this system offers the capability to streamline design and

experimentation which is vital for developing future, more effective cleaning procedures and anti-foulant research.

Standard QCM-D protocol was followed to perform the preliminary fouling analysis using neat gold sensors. This protocol consisted of performing pre- and post-system cleanings by first pumping approximately 20mL of 2% Hellmanex II through the flow tubes leading to each module containing a designated cleaning sensor at 0.300mL/min. This process was repeated using 20mL of DI water followed by air until the system was emptied. The cleaning sensors were then removed, dried with nitrogen gas, and placed in a UV/ozone chamber for 10-15 minutes. The other parts of the modules, along with the inlet and outlet flow holes, were also dried with nitrogen.

Chapter II: Results and Discussion

ED Experimentation with Sodium Alginate and Bovine Serum Albumin

ED separation was performed for five different diluate solutions with three trials for each solution. 10g of NaCl was added to each 300 mL of deionized water to reintroduce a controlled number of ions for filtration. One solution was set aside to be the control "Neat NaCl" solution. Our model foulants were added separately to two of the remaining solutions at a concentration of 0.1wt%. A homogeneous mixture was achieved by placing the solution on a hotplate stirrer at 60C for 30 minutes. This process was repeated for the final two solutions, adding 0.25wt% of the model foulants.

For each of solution, and the change in ion concentration of the diluate stream was recorded every 15 minutes for three hours. This process was repeated for the additional trials, and the average change in conductivity was graphed over time (**Fig 4**). This data showed that

increasing the concentration of the model foulants slightly increased the rate at which ions were separated from the solution. To better visualize this, the current efficiency was calculated using the average of the three trials for each experiment (**Table 1**).

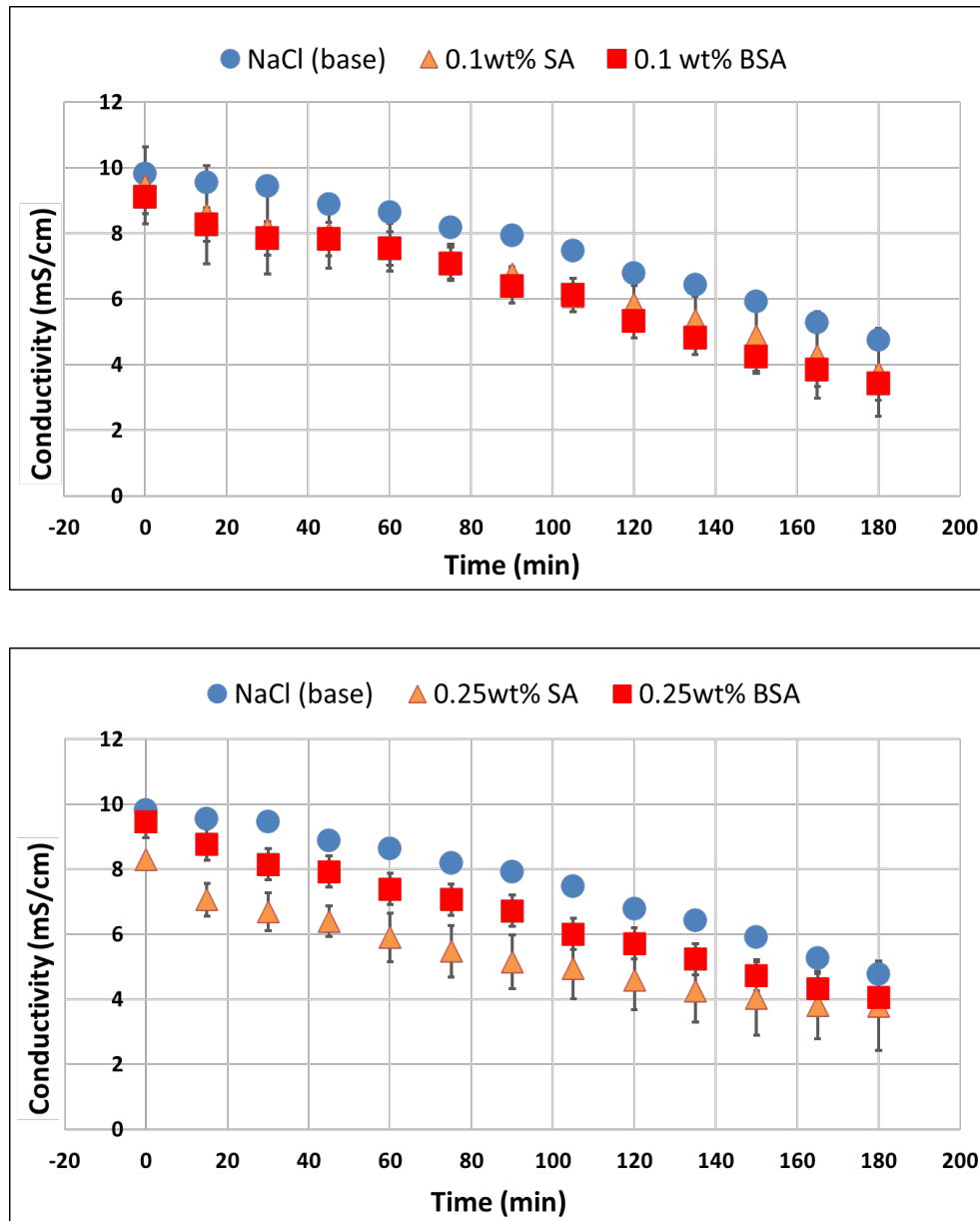


Figure 4: Graphs visualizing the average change in conductivity over time for three trials of each diluate solution during electrolysis experimentation. Solutions with the addition of 0.1wt% SA and BSA (Above) and 0.25wt% SA and BSA (Below) were compared to a neat NaCl solution.

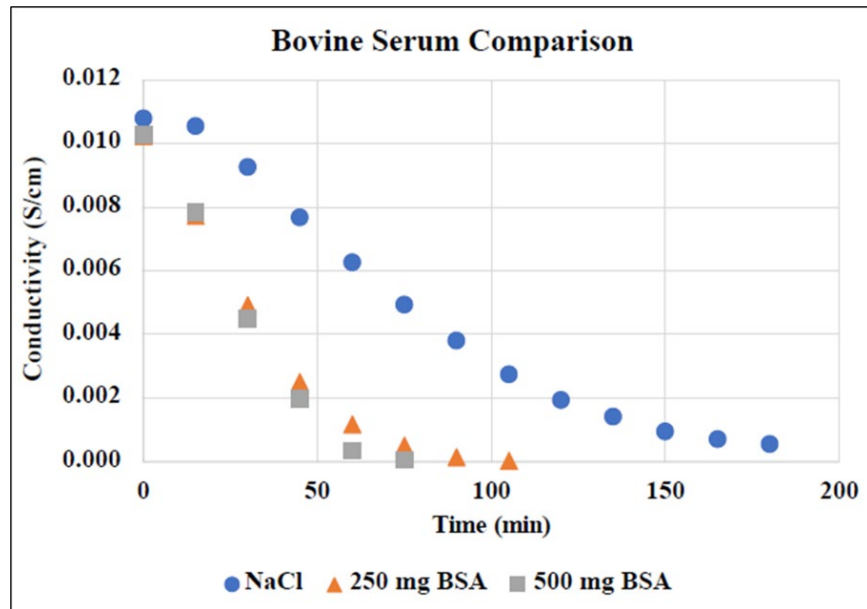
Experiment	Current Efficiency (%)	$\Delta C/t$ (mol/s)
Neat NaCl	37.32 ± 3.13	0.792×10^{-3}
NaCl + 0.1 wt% SA	47.28 ± 9.57	1.003×10^{-3}
NaCl + 0.1 wt% BSA	40.49 ± 1.66	0.859×10^{-3}
NaCl + 0.25 wt% SA	48.18 ± 18.50	1.022×10^{-3}
NaCl + 0.25 wt% BSA	41.48 ± 0.60	0.822×10^{-3}

Table 1: Current efficiency values determined by the average change in concentration for three trials of each diluate solution compared to the total power supplied to the system.

Looking at the results of the experimentation, including uncertainty, the changes in conductivity due to the addition of the foulants are almost negligible. Contrary to the expected outcome, the current efficiency values show that adding the foulants at the chosen concentrations causes an increase in the efficiency of the system rather than limiting ion permutation. One possible reason for this observation is that the foulant concentrations were too low to allow for the development of a foulant layer thick enough to hinder ion transfer. Furthermore, the addition of the foulants could slightly alter the polarity of the solution. This alteration would allow for a more suitable environment for electron exchange and increase the potential of the electrical gradient.

Based on prior research and known industrial challenges, foulant levels often far exceed this unknown threshold and start to reduce system efficiency. A previous study at the University of Mississippi performed similar ED experimentation with SA and BSA [12]. In this study, they noted similar findings regarding low concentrations of foulants assisting the separation rate of

the system. However, at higher concentrations, the efficiency started to decrease (**Fig. 5**). The results show that the highest concentration of SA (500mg) greatly limited the separation process, resulting in the final concentration being about 300% greater than that of the other experiments. Interestingly, adding BSA at the same concentration still has no adverse effect on the system. This data shows the complexity of the fouling process, the interactions occurring at the membrane surface, and the unique relationship between specific foulant properties and the efficiency of ED systems.



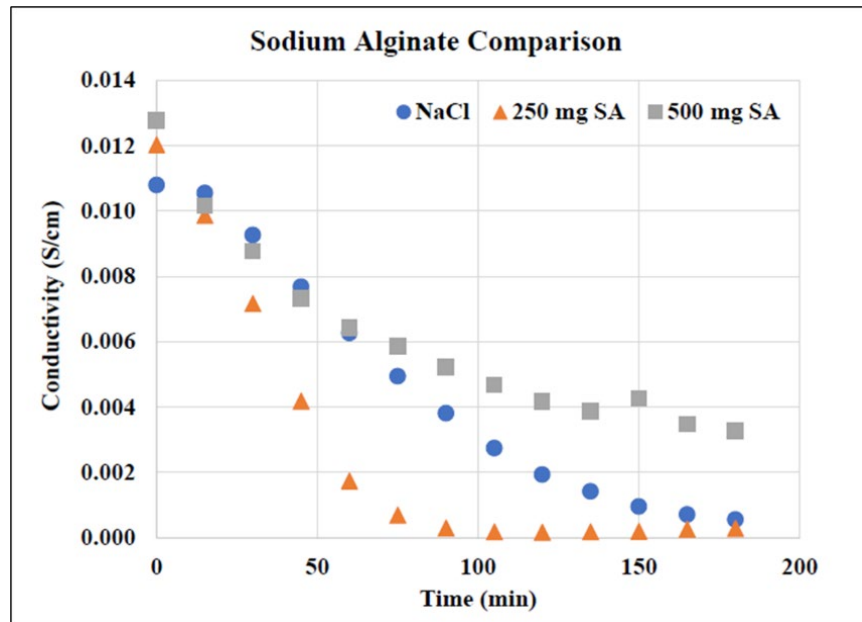


Figure 5: Electrodialysis results with the addition of BSA and SA used with permission from Edward M. et al. [12]. **(Top)** The addition of BSA at amounts of 250 and 500 mg causes an increase in the rate of ion separation. **(Bottom)** Increasing the amount of SA from 250 to 500 mg significantly reduces the ion separation rate.

Development of IEM on Gold QCM-D Sensor

Little prior research is dedicated to understanding specific foulant layer characteristics and molecular interactions at the membrane's surface in ED systems. A better understanding of these factors would contribute significantly to improving the effectiveness of this invaluable water filtration system. The unique abilities of the QCM-D give it the potential to perform rapid real-time analysis of the fouling process with adjustable variables such as temperature, flow rate, and feed water solution. These features make it a perfect candidate for rapid, specialized fouling experimentation and analysis.

A methodology for developing a mock IEM on the surface of a suitable QCM-D sensor would first need to be established before any experimentation could be completed. Standard gold QCM-D sensors were selected as the base for the mock IEM in this study. The mock IEM was built by depositing drops of Fumion anion exchange membrane in solution onto the sensor

surfaces using a Laurell Technologies' spin coater with a QCM-D sensor attachment. The AEM in the solution was first diluted down to a 1wt% solution. Around five drops of this solution were applied to the sensor surface using a pipette until the surface was saturated. The spin coater was then run for 30 seconds, followed by a 30-second rest period. This process was repeated until 30 drops of solution had been deposited on the sensor's surface. The sensor was then allowed to dry completely overnight.

This mock IEM coating procedure was performed on four different gold sensors with slight variations to the coating technique. For the first two sensors, a total of 150 drops of AEM in solution was applied over five days. One of these 150 drop sensors was allowed to dry at room temperature overnight while the other was placed in an oven at 60°C. The following two sensors underwent the same procedure; however, the total number of drops of the AEM in solution was increased to 300. Each day, before the sensors were coated, they were weighed to determine their change in mass over time (**Fig. 6**).

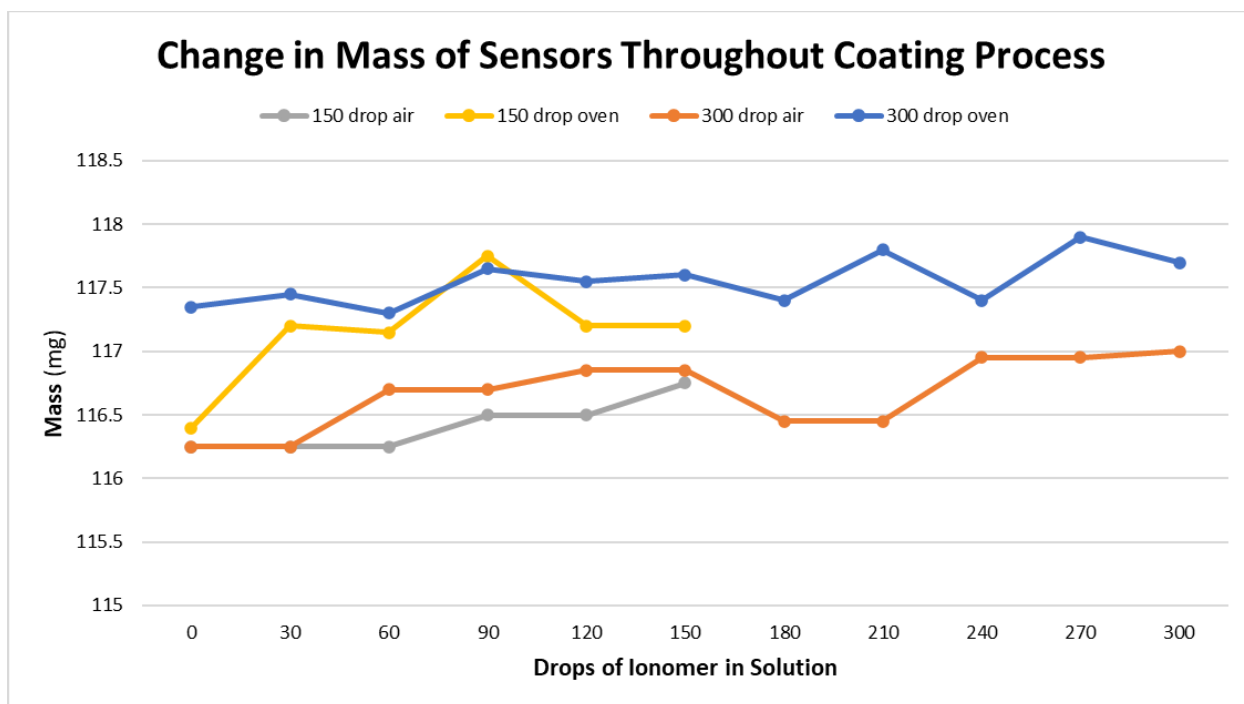


Figure 6: Graph showing the change in mass over time of the QCM-D sensors after solution deposition.

Based on this data, portions of the mock IEM layer were removed from the surface throughout the coating process. This loss of the membrane layer could be due to weak bond interactions between the IEM and the gold surface. Precoating the sensors with a buffer layer in future studies may facilitate the development of a more robust and uniform mock IEM layer. Additionally, it may prove beneficial to utilize a scale that can more accurately measure changes in mass less than the milligram ($< 10^{-3}$) to prevent the introduction of device error. The final change in mass for the 150 drop - Air dry, 150 drop - Oven dry, 300 drop - Air dry, and 300 drop - Oven dry were 0.5mg, 0.8mg, 0.75mg, and 0.35mg, respectively.

Visualization and Validation of Mock IEM

Several validation methods were employed to confirm the formation of the mock IEM and determine the accuracy of specific properties when compared to standard IEMs. First, the mock IEM layer was observed using a Keyence microscope at 250x magnification (**Fig. 7**).

These images show apparent differences in the surface environment of the sensors before and after IEM solution deposition using the spin coater. There appears to be a significant variation in the uniformity of the mock layer, which may affect the accuracy of QCM-D experimentation.

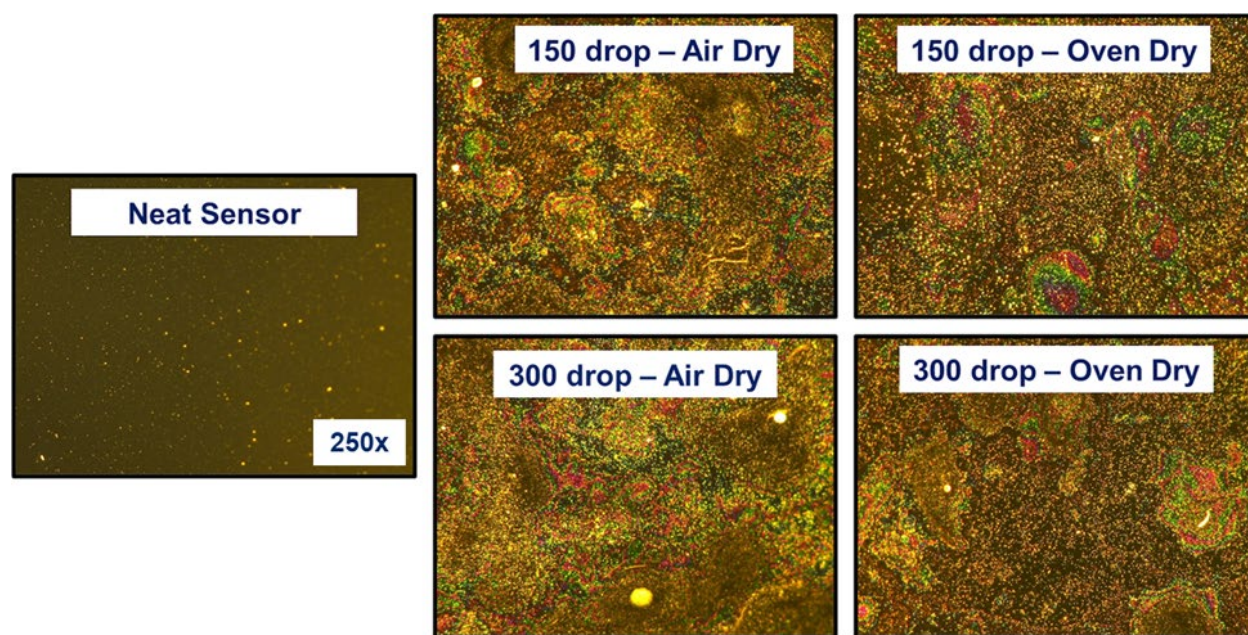


Figure 7: Images of the QCM-D gold sensor surfaces after the mock IEM coating procedure was completed. These images were acquired using a Keyence microscope under 250x magnification.

AFM analysis was performed on each sensor with $5 \times 5 \mu\text{m}$ and $20 \times 20 \mu\text{m}$ resolutions to better understand and visualize the surface topography. The results were analyzed using the Gwyddion software to produce the following 3D images of the mock IEM layer (**Fig. 8**). Looking at the images; there is a significant increase in the vertical z-scale signifying the addition of a material layer on the sensor's surface. Furthermore, the predicted clustering of the

deposited material can be seen more easily across each sensor, particularly for the 150-drop - Air dry and 150-drop - Oven dry samples.

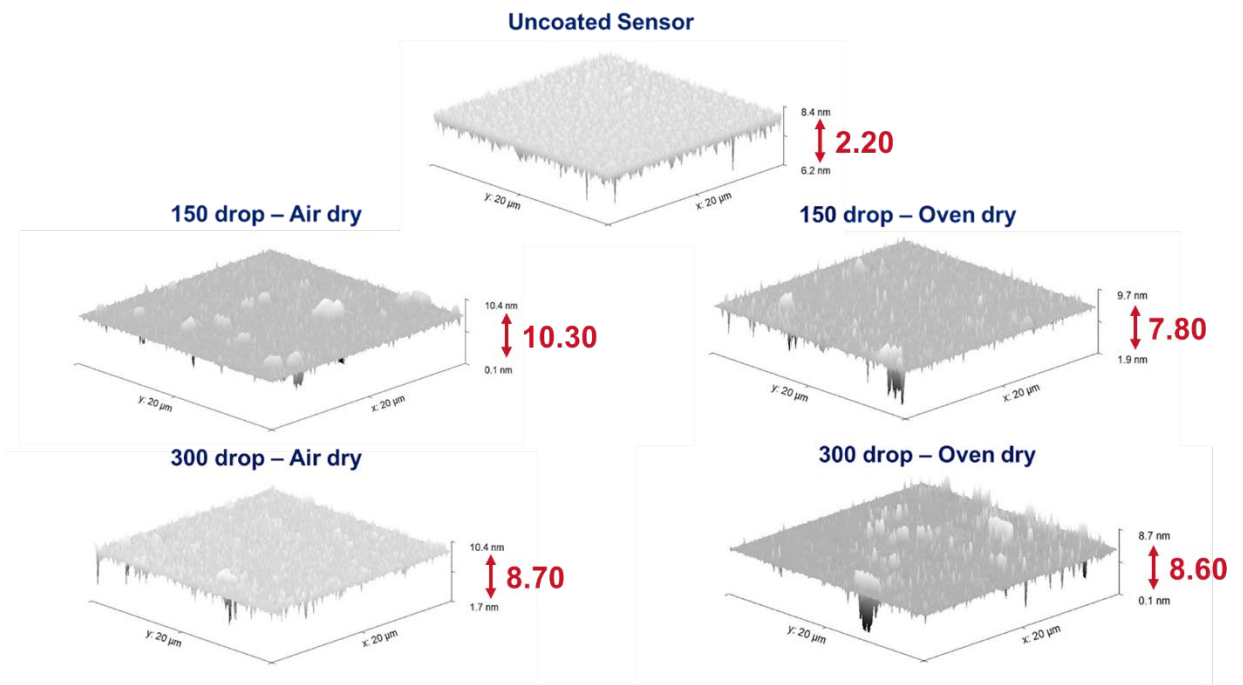
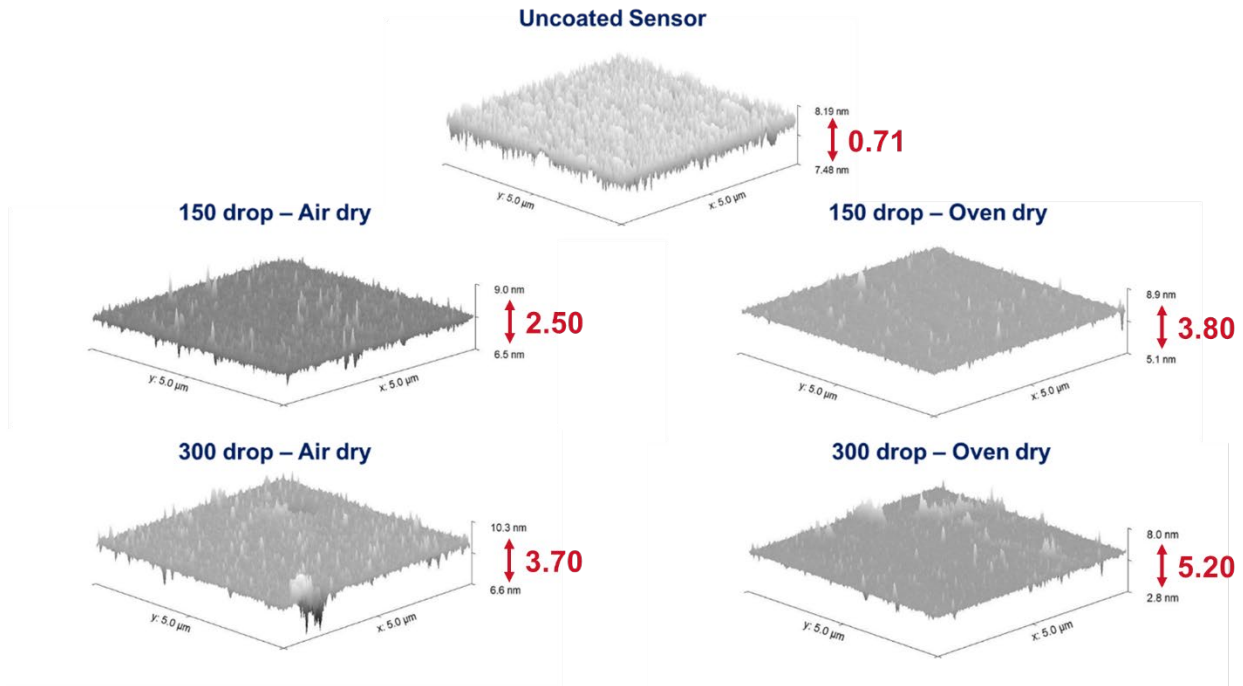


Figure 8: AFM results from 5x5 μm (**Above**) and 20x20 μm (**Below**) areas of uncoated and coated sensor surfaces. The z-axis gives the difference between the highest and lowest points along the surface.

To determine the consistency of the membrane layer, the roughness average (Ra) value was calculated using the height values for each surface's peaks and valleys. The following equation was used to calculate the Ra values where **L** is the evaluation length and **r_j** is the profile height function:

$$R_a = \frac{1}{N} \sum_{j=1}^N r_j \quad (4)$$

This evaluation was completed using the Gwyddion software's "Calculate Roughness Parameters" function along a diagonal slice of the 2D surface image to limit skewed analysis due to the material clustering (**Fig 9**). This data was extracted and compiled in **Table 2**. Comparing the total amount of IEM in solution spin-coated onto the sensor's surface, the average roughness values significantly decrease except for the 5x5 μm 150 drop - Air dry sample. This outlier is likely due to very few of the sporadically distributed clusters falling within that particular diagonal slice. Overall, these results coincide with the visual analysis of more significant clustering for the 150 drop samples leading to more uneven surface topography. Additionally, the oven-dried sensors tend to have a lower roughness average than the air-dried sensors.

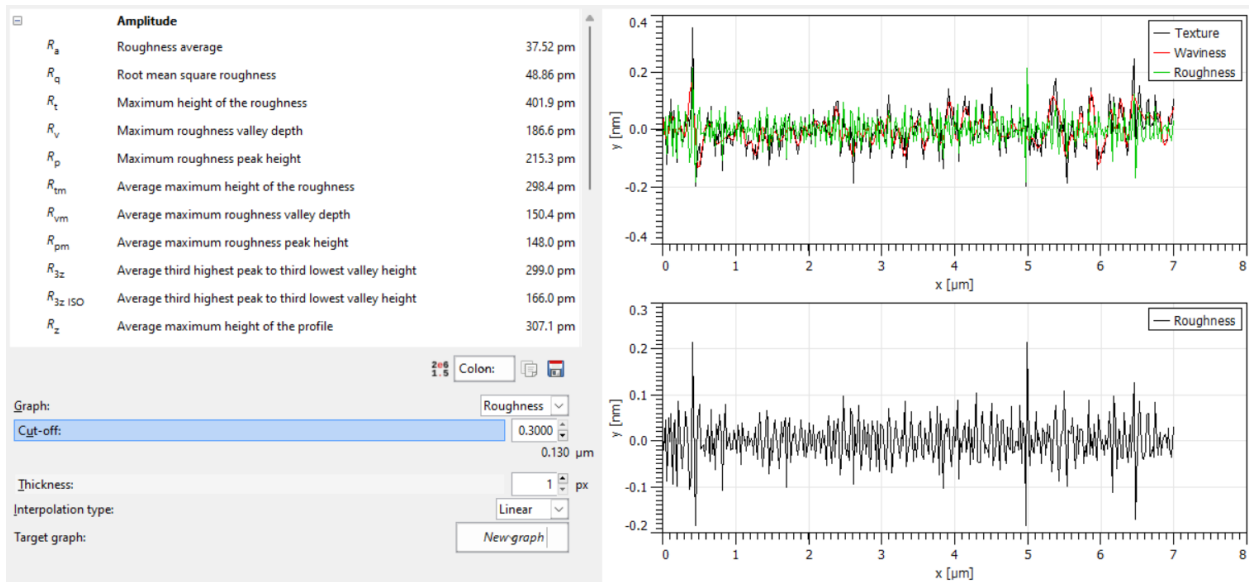
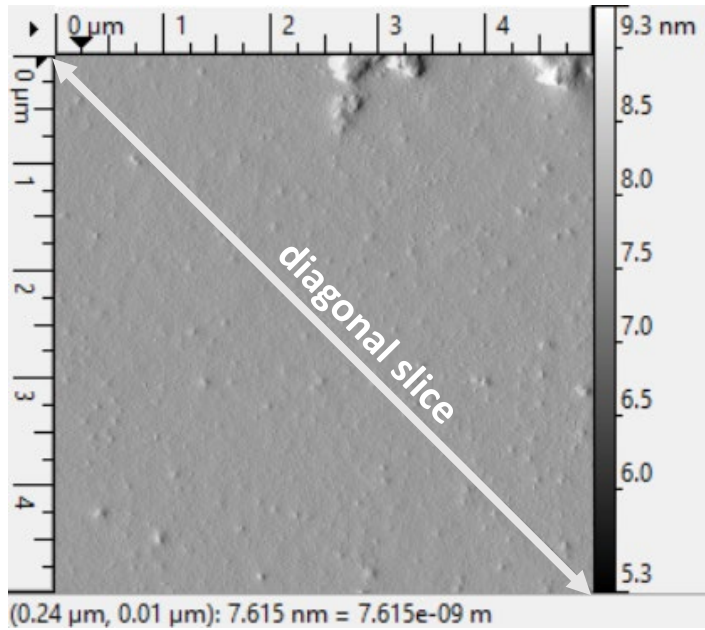


Figure 9: Sample images from the Gwyddion software used to calculate the roughness average value for the 150-drop – Air dry sensor. **(Above)** The 2D surface image with a line representing the drawn cross-section. **(Below)** Gwyddion's roughness parameters page with roughness data for the sample.

Coating Method	Roughness Average (R_a [μm])	
	5x5 μm Area	20x20 μm Area
Uncoated	22.79	51.55
150 drop – Air dry	37.23	140.0
150 drop – Oven dry	65.65	106.6
300 drop – Air dry	55.06	87.25
300 drop – Oven dry	51.40	62.86

Table 2: Roughness average (R_a) values for an uncoated and the four mock IEM-coated sensors calculated from a diagonal slice across the sensor's surface.

CA analysis was performed to further compare the physical properties of the mock IEMs to standard IEMs. A drop of distilled (DI) water was placed onto the surface of each coated sensor. The wettability of the sensor's surface was calculated by the angle created at the liquid-solid interface using the Attension Theta Flex (**Fig. 9**). Except for the 150 drop - Air dry sample, which increased around 7.0° , the contact angle for each sensor's surface decreased more than 10.0° . Common AEMs utilized in water filtration systems have a contact angle value of $\sim 54.0^\circ$ [13, 14]. The 300 drop - Air dry value was observed to be closest to the expected value with a measurement of 58.0 - 59.0° . Variations in these values could be due to errors or contamination throughout the coating process and uneven surface coating.

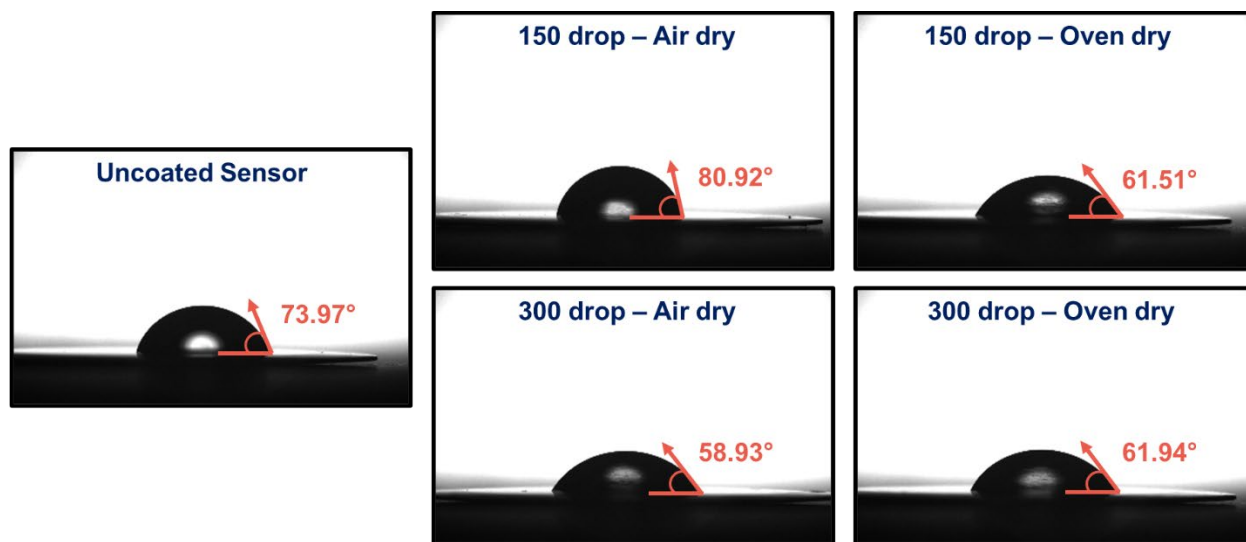


Figure 10: Images displaying the contact angle value for each coated sensor and an uncoated gold sensor. The known literature value for the contact angle of AEM is $\sim 54^\circ$ [13, 14].

Preliminary QCM-D Experimentation with Uncoated Sensors

Some initial experimentation was conducted to test procedure viability in the QCM-D. Uncoated gold sensors were used for these experiments, and our 0.1wt% foulant solutions were run over the sensor's surfaces. A saltwater solution with no foulant concentration was also used as a baseline. The amount of particle deposition for each solution was measured over time using the QCM-D's QSense software and compiled in **Fig. 10**. These results show a clear delineation between the total amount and rate of particle deposition for each solution. It also shows differences in the amount of particle layer residue left on the surface after a DI water wash was run through the system. Based on this preliminary analysis, the QCM-D can quickly measure and visualize case-specific foulant layer properties even at relatively low concentrations.

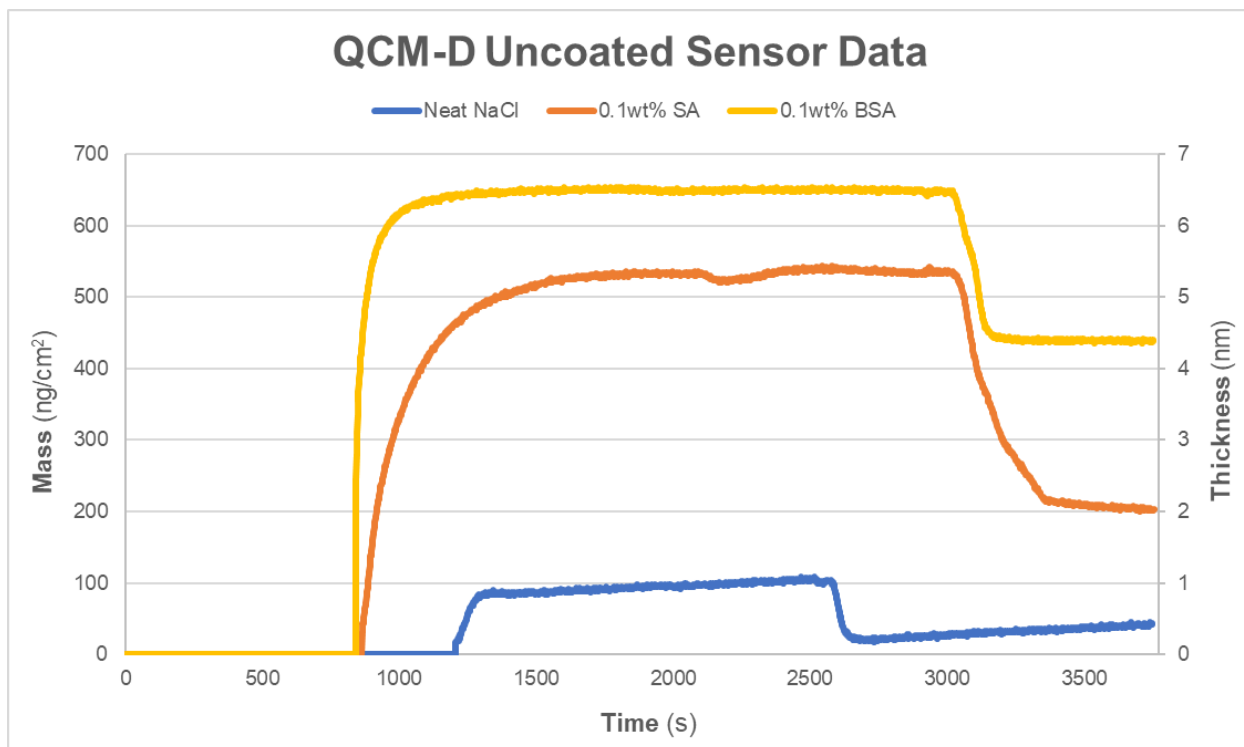


Figure 11: Surface interaction data between uncoated gold QCM-D sensors with solutions containing neat NaCl (**Blue**), Sodium Alginate (**Orange**), and Bovine Serum Albumin (**Yellow**) at a constant flow rate of 0.150mL/s. After the interaction data was collected, an ultrapure water rinse was supplied to the system. The time values for the neat NaCl run were scaled to fit with the other data.

Chapter III: Conclusion and Future Work

Based on the experimentation performed in this study, previous studies, and industrial use of ED systems, organic fouling is a complex issue that can cause significant complications throughout the filtration process. This study sought to better understand foulant layer properties and develop a novel methodology for streamlining future foulant analysis and anti-foulant research in ED systems. The QCM-D was proposed as a device capable of achieving these objectives due to its real-time particle deposition measurement capabilities and straightforward analysis and comparison across multiple studies. The experimental setup for this device also

allows for modifiable factors such as independent channel feed water concentrations, flow rate, and temperature.

A novel methodology was developed for building a mock IEM on the surface of the standard gold QCM-D sensor to test the validity of the QCM-D as a tool for foulant analysis. This was achieved by performing a spin coating procedure with AEM in solution. Variations in the amount of solution applied and drying technique were conducted to determine if these factors affected the accuracy of the developed layer when compared to standard IEMs. The physical properties of the mock layer were analyzed using AFM and CA analysis. Based on these results, increasing the amount of AEM solution applied caused a decrease in the average roughness and the development of a more uniform membrane layer. Drying the sensors in an oven versus at room temperature also appeared to reduce membrane clustering; however, the wettability value was further from the expected value. Optimization of the coating methodology with additional sensors may prove beneficial in further improving the accuracy and homogeneity of the mock IEM layer.

The following steps for this research are to perform basic QCM-D experimentation with the coated sensors and determine the integrity of the mock IEM layer. If the coating is removed, it may be necessary to apply a pre-treatment layer before spin coating to strengthen the bonding of the mock IEM to the sensor's surface. Once there is no coating loss, foulant analysis can be performed with the addition of BSA and SA to the experimental solution at specific concentrations. Utilizing the QCM-D analysis software, the fouling profiles for these two model foulants can be analyzed and recorded for comparison in additional studies.

The tunability of this research shows its potential of becoming a vital new technique for advancing water filtration processes. Running solutions from different feed sources under

adjustable experimental conditions allows for case-specific foulant layer analysis. This technique would be ideal rather than the expensive and destructive membrane autopsies commonly performed today. Additionally, analysis of properties such as the rate of fouling and the threshold for system hindrance using the QCM-D allow for a greater understanding of fouling mechanisms. This information would be valuable to help maximize the system's current efficiency and determine the optimal cleaning rate.

This novel coating methodology would also streamline future foulant prevention research. Several concepts that could be further tested may be the addition of current anti-fouling coatings onto the mock IEM to determine their effectiveness given a specific feed water composition. This simple coating process also facilitates developing and testing new specialized anti-foulant coatings. Furthermore, cleaning solutions may also be run through the system after foulant deposition, and their effects on foulant layer removal could be easily analyzed and compared.

Membrane fouling is an issue that has been plaguing the membrane filtration industry for decades and frequently leads to costly and time-consuming system repairs. The results from this study show great potential for the QCM-D to become a valuable tool in limiting complications caused by fouling by increasing understanding of foulant mechanisms and facilitating the development of preventative measures. This foulant analysis technique could also be translated to other membrane filtration processes such as reverse osmosis, nanofiltration, and ultrafiltration. Addressing these issues would significantly benefit process performance and dramatically reduce unnecessary expenses and complications. As water issues increase in severity across the United States and the world, improving the efficiency of these water filtration systems would play a key role in combating water scarcity and ensuring the availability of clean water.

LIST OF REFERENCES

1. Strathmann, H. (2010). Electrodialysis, a mature technology with a multitude of new applications. *Desalination*, 264(3).
2. Xu, T. (2005). Ion exchange membranes: State of their development and perspective. *Journal of Membrane Science*, 263(1–2).
3. Bleha, M., & Tishchenk, G. (1992). Characteristic of the Critical State of Membranes in ED-Desalination of Milk Whey. In *Desalination* (Vol. 86).
4. Mikhaylin, S., & Bazinet, L. (2016). Fouling on ion-exchange membranes: Classification, characterization and strategies of prevention and control. In *Advances in Colloid and Interface Science* (Vol. 229, pp. 34–56). Elsevier.
5. Sadhwani, J. J., & Vezab, J. M. (2001). DESALINATION Cleaning tests for seawater reverse osmosis membranes. In *Desalination* (Vol. 139).
6. Arnal, J., Garcia-Fayos B, & Ma S. (2011). *Expanding Issues in Desalination* (R. Ning, Ed.). InTech.
7. Liu, G., & Zhang, G. (2013). *Basic Principles of QCM-D*.
8. Park, J., Lee, S., You, J., Park, S., Ahn, Y., Jung, W., & Cho, K. H. (2018). Evaluation of fouling in nanofiltration for desalination using a resistance-in-series model and optical coherence tomography. *Science of The Total Environment*, 642.
9. Akamatsu, K., Kagami, Y., & Nakao, S. (2020). Effect of BSA and sodium alginate adsorption on decline of filtrate flux through polyethylene microfiltration membranes. *Journal of Membrane Science*, 594.
10. Sweity, A., Ying, W., Ali-Shtayeh, M. S., Yang, F., Bick, A., Oron, G., & Herzberg, M. (2011). Relation between EPS adherence, viscoelastic properties, and MBR operation: Biofouling study with QCM-D. *Water Research*, 45(19), 6430–6440.
11. Huellemeier, H. A., Eren, N. M., Payne, T. D., Schultz, Z. D., & Heldman, D. R. (2022). Monitoring and Characterization of Milk Fouling on Stainless Steel Using a High-Pressure High-Temperature Quartz Crystal Microbalance with Dissipation. *Langmuir*, 38(31), 9466–9480.
12. Edwards, M. J. (2019). *INVESTIGATION OF FOULING MECHANISMS ON ION EXCHANGE MEMBRANES DURING ELECTROLYTIC SEPARATIONS*.
13. Nagarale, R. K., Shahi, V. K., Schubert, R., Rangarajan, R., & Mehnert, R. (2004). Development of urethane acrylate composite ion-exchange membranes and their electrochemical characterization. *Journal of Colloid and Interface Science*, 270(2).

14. Vasil'eva, V. I., Pismenskaya, N. D., Akberova, E. M., & Nebavskaya, K. A. (2014). Effect of thermochemical treatment on the surface morphology and hydrophobicity of heterogeneous ion-exchange membranes. *Russian Journal of Physical Chemistry A*, 88(8).

LIST OF EQUATIONS

Equation 1: Sauerbrey Relation

$$\Delta m = -C \times \frac{\Delta f}{n}$$

C – mass-sensitivity constant

n – chosen harmonic Frequency

Δf – change in frequency

Equation 2: Piezoelectric Material's Mass-Sensitivity Constant

$$C = \frac{v_q \times p_q}{2(f_0)^2}$$

v_q – shear wave velocity

f_0 – fundamental resonance frequency

p_q – density

Equation 3: Current Efficiency

$$\xi = \frac{zFV \times (C_i - C_f)}{t \times l}$$

C_i – initial ion concentration

F – Faraday's Constant

V – diluate volume

$$\xi = \frac{\text{energy consumed}}{\text{energy supplied}}$$

C_f – final ion concentration

I – average current

s – separation time

z – ion valence

Equation 4: Roughness Average

$$R_a = \frac{1}{N} \sum_{j=1}^N r_j$$

L – evaluation length

r_j – profile height function

APPENDIX

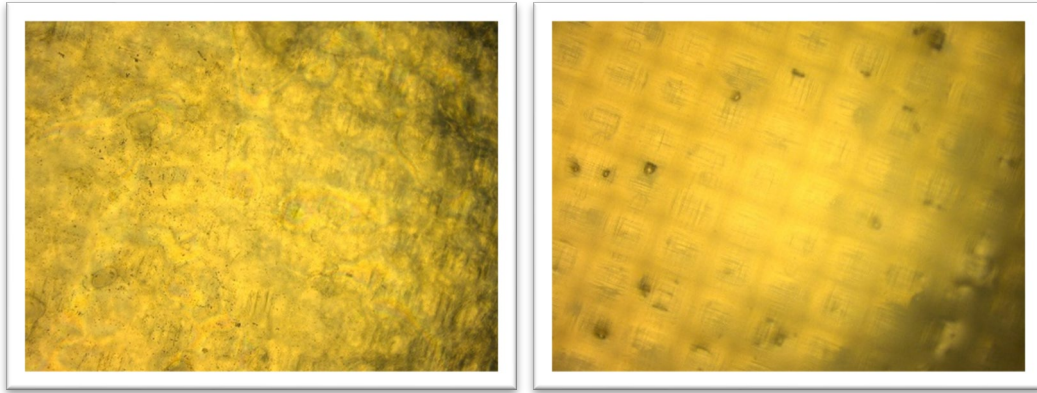


Figure 12: Images comparing the surface of a membrane fouled by the SA solution (**Left**) to an uncontaminated membrane (**Right**) after completing an ED cycle using the Keyence microscope.

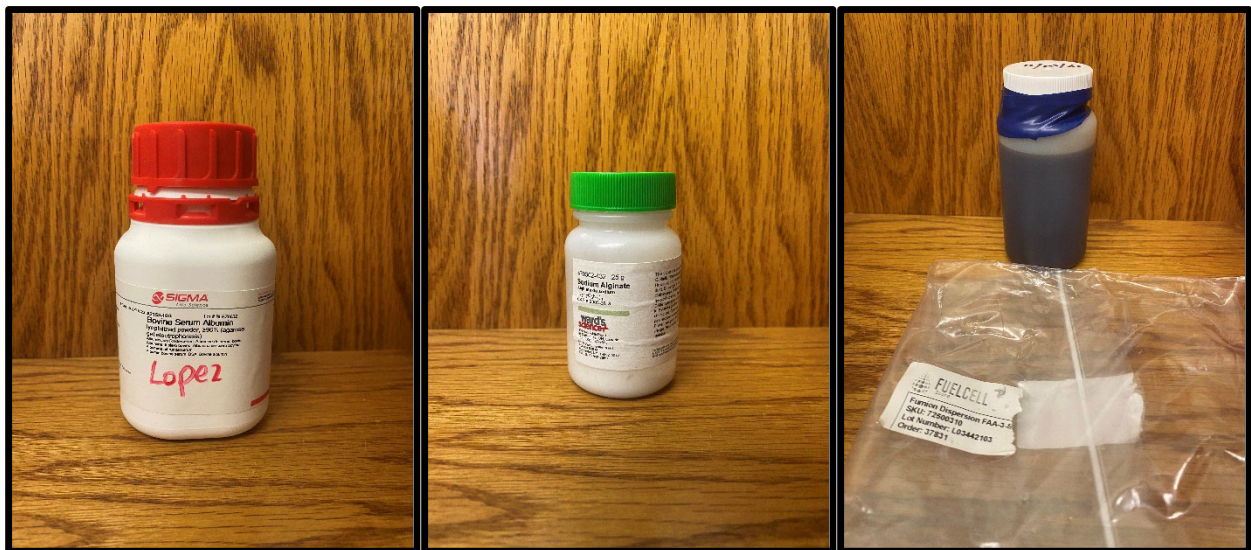


Figure 13: Images of the two model foulants, BSA and SA (**Left, Middle**), and the Fumion® anion exchange in solution (**Right**) with production information.

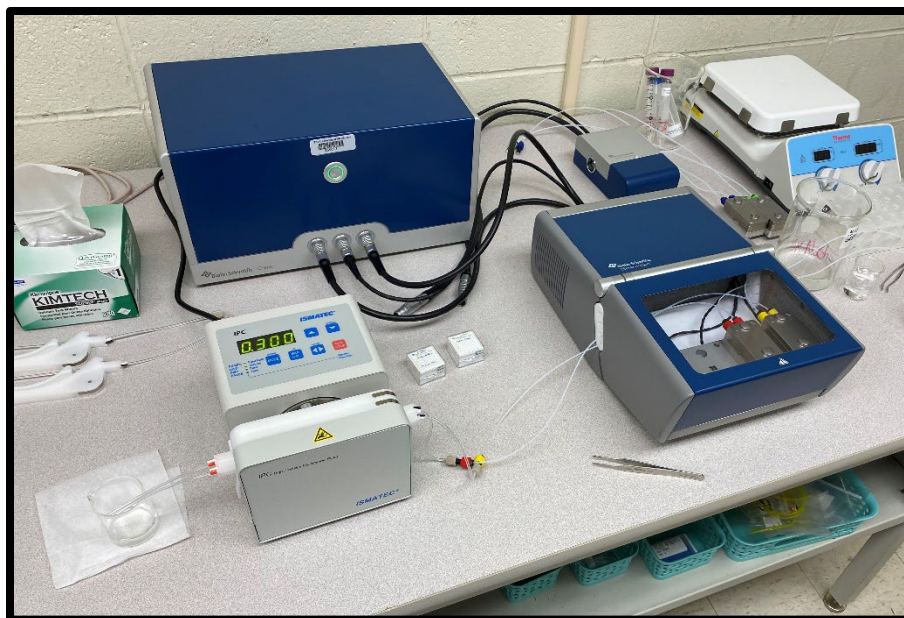


Figure 14: QCM-D experimental set up for standard fluid flow procedures.



Figure 15: Spin-coater with QCM-D sensor attachment and vacuum pump experimental set up.